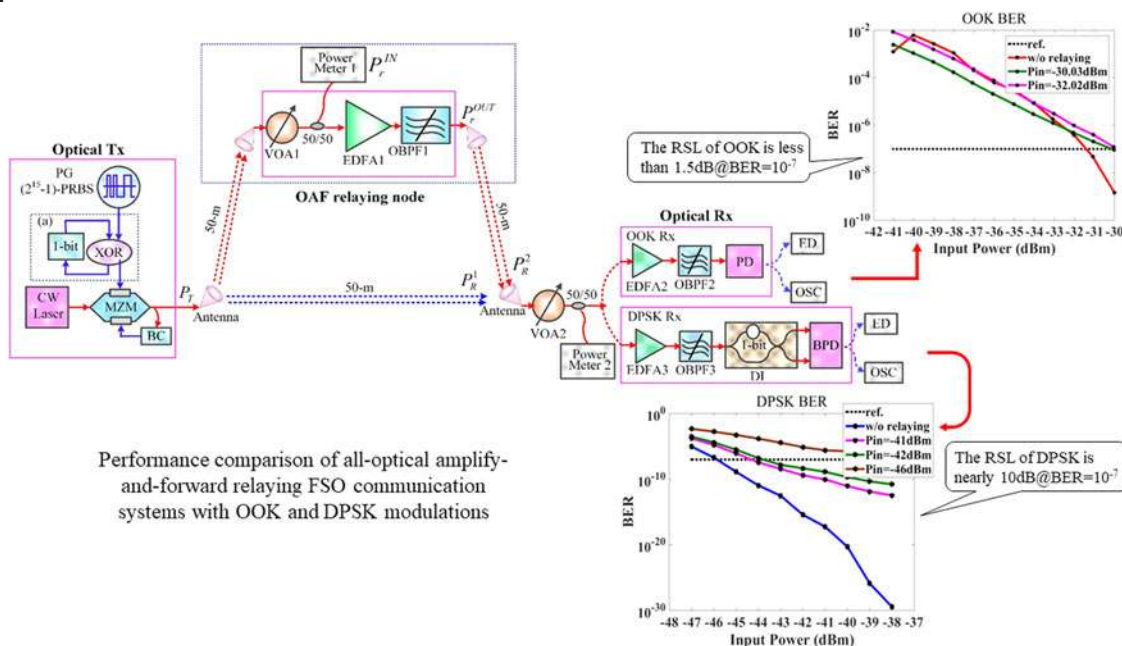


# Performance Comparison of All-Optical Amplify-and-Forward Relaying FSO Communication Systems With OOK and DPSK Modulations

Volume 10, Number 4, August 2018

Xinning Huang  
 Xiaoping Xie  
 Jiazheng Song  
 Tao Duan  
 Hui Hu  
 Xin Xu  
 Yulong Su



DOI: 10.1109/JPHOT.2018.2852301  
 1943-0655 © 2018 IEEE

# Performance Comparison of All-Optical Amplify-and-Forward Relaying FSO Communication Systems With OOK and DPSK Modulations

Xinning Huang <sup>1,2</sup>, Xiaoping Xie,<sup>2</sup> Jiazheng Song,<sup>2</sup> Tao Duan,<sup>2</sup>  
Hui Hu,<sup>2</sup> Xin Xu,<sup>3</sup> and Yulong Su<sup>2</sup>

<sup>1</sup>University of Chinese Academy of Sciences, Beijing 100049, China

<sup>2</sup>State Key Laboratory of Transient Optics and Photonics, Xi'an Institute of Optics and Precision Mechanics of CAS, Shaanxi 710119, China

<sup>3</sup>Hefei University of Technology, Anhui 230009, China

DOI:10.1109/JPHOT.2018.2852301

1943-0655 © 2018 IEEE. Translations and content mining are permitted for academic research only.

Personal use is also permitted, but republication/redistribution requires IEEE permission.

See [http://www.ieee.org/publications\\_standards/publications/rights/index.html](http://www.ieee.org/publications_standards/publications/rights/index.html) for more information.

Manuscript received June 7, 2018; revised June 25, 2018; accepted June 28, 2018. Date of publication July 2, 2018; date of current version July 17, 2018. This work was supported by the National Key Research and Development Program of China (2017YFC0803900, 2017YFC0803909) and National Natural Science Foundation of China (51705121). Corresponding author: Yulong Su (e-mail: [suyulong@opt.cn](mailto:suyulong@opt.cn)).

**Abstract:** All-optical amplify-and-forward (OAF) relaying technique can amplify and filter the attenuated optical signal in optical domain, and thus is regarded as a simple way to extend the transmission distance of free-space optical (FSO) communication systems. At the relaying node, however, the incident background radiation and the amplified spontaneous emission noise of the deployed erbium-doped fiber amplifier will deteriorate the optical signal-to-noise, therefore causing the degradation of the system's bit error ratio (BER). In this paper, we perform simulations and experiments on FSO system with on-off keying (OOK) and differential phase-shift keying (DPSK) signals, focusing on the receiving sensitivity loss (RSL) of the OAF-assisted dual-hop system. Taking the BER level of  $10^{-7}$  as the reference, we find that the DPSK system suffers more than 8 dB RSL at the data rate of 5 Gb/s in simulation, while the OOK system gets less than 1 dB RSL at the same data rate. In the following experiments, the obtained results exhibit that RSL of DPSK system is nearly 10 dB, which of OOK system is less than 1.5 dB, shown similarly property to the simulations.

**Index Terms:** Free-space optical communication, all-optical relaying, receiving sensitivity loss, OOK, DPSK.

## 1. Introduction

Free-Space optical (FSO) communication has many advantages such as high bandwidth, license-free and robustness to electromagnetic interference, making it an effective alternative to lots of applications [1]–[5], especially to long-haul high-data-rate transmissions [6]–[8]. However, the conditions of the atmospheric channel limit the reliability of FSO links. The major problem is the severe power loss due to the atmosphere turbulence, long-haul geometrical beam spread and pointing and tracking error [9]–[11], resulting in poor bit-error rate (BER) performance at the receiver, and thus shorting the link range [12].

To increase the link range as well as to optimize the BER of the FSO system, optical relaying-assisted transmission technique is proposed. This technique processes and forwards the transmitted optical signal at intermediate terminals, which are usually called relaying nodes, between the transmitter and the receiver of the communication system. At the relaying nodes, optical signals can be processed in either decode-and-forward (DF) or amplify-and-forward (AF) modes. In DF relaying, the optical signal is firstly demodulated to electrical data, decoded and re-coded in electrical domain, and then re-modulated on an optical carrier to forward [13]. This procedure employs optical-to-electrical (O/E) and electrical-to-optical (E/O) conversions, making the relaying nodes complex and costly, besides, the bandwidth of the electrical processors limit the relaying data-rate. While in AF relaying, the optical signal still experiences O/E and E/O conversions, but the decoding and recoding processes are omitted [14], reducing the demands on high-speed electronic devices and optoelectronic devices.

Since both of the two relaying methods need O/E/O conversion, all-optical relaying techniques, namely all-optical AF (OAF) and optical regenerate-and-forward (ORF), are put forward to simplify the system structure. The OAF utilizes erbium-doped fiber amplifier (EDFA) and optical band-pass filter (OBPF) to enable the relaying bandwidth unlimited [15]–[19], while the ORF adopts nonlinear effect to regenerate the noise-polluted signal [20], [21]. Since the ORF requires that the input optical power should be high enough to trigger the nonlinear effect, and the interactional optical fields should keep a kind of fixed phase relationship to realize the regeneration, the OAF is a preferable simple way to relay the degraded optical signal. Now that the OAF can lengthen the link range, improve the BER performance and enhance the network flexibility by releasing the requirement of line-of-sight (LOS) in the FSO systems, it can be used in many scenarios, for example, disaster relief where the surveillance data is time critical to the command center, inter-satellite link handover when the communication is interrupted or unavailable between the source and the destination, as well as large volumes data transmission between non LOS terminals [22], [23]. However, at the OAF relaying node, the background radiation and the amplified spontaneous emission (ASE) noise of the EDFA should be taken into consideration because they may cause optical signal-to-noise (OSNR) degradation, especially for weak signal after a long-distance transmission.

At the same time, the transmitting information in FSO systems can be modulated on either intensity or phase of an optical carrier, namely on-off keying (OOK) modulation or phase shift keying (PSK) modulation. The OOK signal can be directly detected by a photo-detector, making the receiver structure simpler than PSK (which needs to convert phase message onto intensity before detection). However, the PSK signal requires lower optical power than OOK to achieve the same BER at the receiver. For example, the differential PSK (DPSK) signal with a balanced receiver has 3 dB sensitivity benefit over OOK. Moreover, DPSK receiver needs neither local laser nor optical phase lock loop, simplifying the receiver structure and making it easy to be deployed in space applications.

There are plenty of OAF relaying studies which, under certain models of atmospheric turbulence, mainly focus on the theoretical derivation of the outage probability or optical signal to noise ratio (OSNR), and system performance based on numerical analyzing are demonstrated. However, the receiving sensitivity loss (RSL) caused by the OAF relaying node are barely discussed. In this paper, the performance of an OAF relaying-assisted FSO communication system with OOK and DPSK signals are evaluated. The impacts of the ASE noise from the EDFA and the optical power fading caused by the atmospheric channel are mainly considered, and RSLs of the OOK and DPSK dual-hop FSO systems are respectively researched through simulations and experiments.

## 2. System Model

The schematic diagram of a dual-hop FSO communication system is shown in Fig. 1, and the OAF relaying procedure which we primarily discuss in this paper is demonstrated in inset (b).

In the OAF relaying-assisted FSO system, the output optical field of the transmitter is:

$$E_T(t) = E_0 \cos(2\pi\nu_0 t) \quad (1)$$

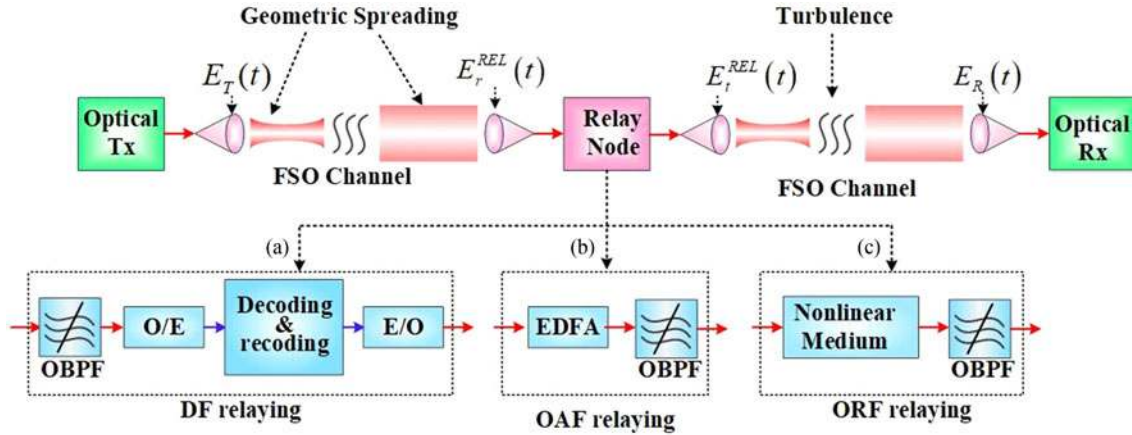


Fig. 1. Schematic diagram of a dual-hop FSO communication system, with inset. (a) DF relaying diagram, inset. (b) OAF relaying and inset. (c) ORF relaying diagram respectively. Tx: transmitter, Rx: receiver, OBPF: optical band-pass filter.

where  $E_0$  is the electrical field amplitude and  $\nu_0$  is the center frequency of the optical light source respectively. After a section of free space transmission, the received optical field  $E_r^{REL}(t)$  at the relaying node can be written as:

$$E_r^{REL}(t) = \alpha_1 E_T(t) + E_{b1}(t) \quad (2)$$

where  $\alpha_1$  represents the transmission loss caused by antenna optics of Tx and Rx, geometrical spread, atmospheric attenuation, and coupling from space to single mode fiber (SMF), and  $E_{b1}(t)$  is the background radiation field between the transmitter and the relaying node.

At the relaying node, the optical signal is amplified by an EDFA (with gain  $G$  and ASE noise  $E_{ASE}(t)$ ), matching filtered by an OBPF to remove the out-band noise and then re-transmitted into another length of free space. When the relayed signal finally arrives at the receiver, the optical field is

$$E_R(t) = G\alpha_1\alpha_2 E_T(t) + G\alpha_2 E_{b1}(t) + \alpha_2 E_{ASE}(t) + E_{b2}(t) \quad (3)$$

where  $\alpha_2$  is the transmission loss similar to  $\alpha_1$  and  $E_{b2}(t)$  is the background radiation between the relaying node and the receiver.

At the receiver, the received optical signal is demodulated and detected by a photo-detector for data recovery. The photocurrent  $I_R(t)$  generated by the detector is directly proportional to the square of the input optical field:

$$I_R(t) = \frac{e\eta}{h\nu_0} E_R^2(t) \quad (4)$$

where  $e = 1.6 \times 10^{-19}C$  is the charge of an electron,  $\eta$  is the photo-detector efficiency, and  $h$  is the Planck constant. Combing (1)–(4) we can obtain:

$$\begin{aligned} I_R(t) = & R [G^2\alpha_1^2\alpha_2^2 E_T^2(t) + G^2\alpha_2^2 E_{b1}^2(t) + \alpha_2^2 E_{ASE}^2(t) + E_{b2}^2(t)] \\ & + R [2G^2\alpha_1\alpha_2^2 E_{b1}(t) + 2G\alpha_1\alpha_2^2 E_{ASE}(t) + 2G\alpha_1\alpha_2 E_{b2}(t)] E_T(t) \\ & + R [2G\alpha_2^2 E_{b1}(t) + 2\alpha_2 E_{b2}(t)] E_{ASE}(t) \\ & + 2RG\alpha_2 E_{b1}(t) E_{b2}(t) \end{aligned} \quad (5)$$

where  $R = e\eta/h\nu_0$ . Equation (5) indicates that the photocurrent at the receiver contains not only the useful information  $E_T^2(t)$ , but also other components such as the background radiation  $E_{bi}^2(t)$  ( $i = 1, 2$ ), the ASE noise  $E_{ASE}^2(t)$  and the various beat noise. All of these unwanted photocurrent

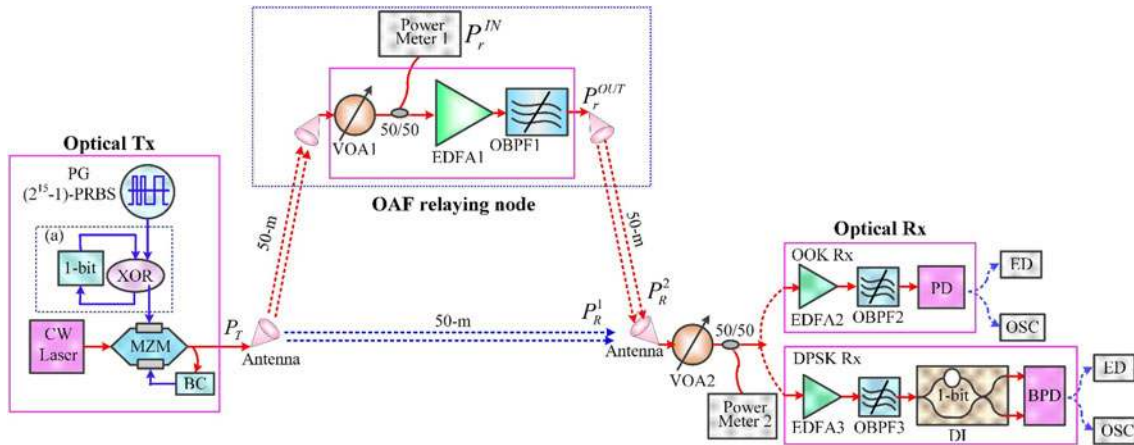


Fig. 2. Simulation and experimental setup of the dual-hop OAF relaying-assisted FSO communication system. CW: continuous-wave, PRBS: pseudorandom binary sequence, PG: pattern generator, BC: bias controller, MZM: Mach-Zehnder modulator, BPD: balanced photodetector, ED: error detector, OSC: oscilloscope.

components will deteriorate the system BER performance, resulting in a poor receiving sensitivity. The influences of the undesired components on the OOK and DPSK dual-hop FSO system are studied in the next section.

### 3. Simulation and Experimental Results

In this section, we carry out simulations and experiments on the OAF relaying-assisted dual-hop FSO communication system, and mainly focus on the RSL of OOK and DPSK systems. The system configuration is illustrated in Fig. 2, and the RSLs of both OOK and DPSK are measured by the following three steps. 1) Receiving sensitivity of the no-relaying (denoted as  $P_R^1$ ) system is measured at a given BER reference, 2) Receiving sensitivity of the OAF relaying-assisted system (denoted as  $P_R^2$ ) is measured at the same BER reference and 3) RSL defined as the difference between  $P_R^1$  and  $P_R^2$  is calculated.

At the transmitter, the OOK and the DPSK share the laser source and the Mach-Zehnder modulator (MZM). The differential encoding (inset (a)) is off for OOK and on for DPSK. After a 50-m free space transmission, the optical signal arrived at the relaying node is amplified by an EDFA, matching filtered by an OBPF and re-transmitted through the other 50-m free space distance to finally arrive at the receiver. Then the OOK signal is directly detected by a photo-detector (PD), while the DPSK signal is firstly demodulated by a 1-bit delay-line interferometer (DI) and then detected by a balanced photo-detector (BPD). Pre-amplifier and filter are used both for OOK and DPSK.

The optical power loss caused by the atmospheric transmission (including optics loss, atmospheric attenuation, geometrical loss, and coupling loss) is primarily considered, and variable optical attenuators (VOAs) are used to simulate the practical optical power attenuation from the transmitter to the relaying node (VOA1), and from the relaying node to the receiver (VOA2). The link budget taking the static loss into account is present in Table 1, in which the atmospheric loss is designed for FSO communication between an airborne terminal (18 to 27-km altitude range) in the stratosphere and an optical ground station [24], and the geometrical loss is calculated by equation (6) [25].

$$Loss_{geo} = 20 \lg \left[ \frac{\sqrt{r_0^2 + (\theta_t z)^2}}{\sqrt{2} R_r} \right] \quad (6)$$

TABLE 1  
FSO System Link Budget

Parameters	Value	Unit
Wavelength	1550.52	nm
Tx Beam Divergence (Half-angle)	0.10	mrad
Rx Aperture Diameter	10.00	mm
Focal Length	50.00	mm
<b>Static Parameters</b>		
Tx power	0	dBm
Tx Antenna Optics Loss	-2.00	dB
Atmospheric Loss	-6.50	dB
Geometrical Loss	-18.52	dB
Rx-Antenna Optics Loss	-2.00	dB
Rx-Coupling Loss	-3.00	dB
Static Rx-Power	-32.02	dBm

where  $r_0$  is the initial Gaussian beam radius calculated by  $r_0 = 10\lambda/\pi\theta_t$ ,  $\theta_t$  is the half-angle of the beam divergence,  $\lambda$  is the signal wavelength and  $R_r$  is the radius of the receiver optics.

### 3.1 OOK Modulation

In the OOK system, the line-width of the laser source at the transmitter is 10-KHz, the wavelength is 1550.52 nm and the output optical power  $P_T$  is 0 dBm. The data rate of the system is 5-Gb/s. At the relaying node, the EDFA1 works at the auto power controlling (APC) mode with the output power fixed at 10 dBm and the noise figure (NF) at 4.6 dB. The bandwidth of OBPF1 is 0.25 nm. At the receiver, the parameters of the pre-amplifier (EDFA2) and the filter (OBPF2) keep same with that in the relaying node.

*3.1.1 Simulation Results:* We firstly carry out simulations (OptiSystem 11) on the no-relaying OOK system, in which the output optical signal of the transmitter travels in 50-m free space, then is attenuated via VOA2 and received by the receiver. By changing the received optical power  $P_R^1$  through VOA2, we record the BERs at different  $P_R^1$  values and plot the BER curves. The obtained results are shown in Fig. 3. From Fig. 3(c) we can find that in the no-relaying transmission system, the receiving BERs are  $1.781 \times 10^{-20}$  @ -30 dBm,  $2.855 \times 10^{-15}$  @ -31 dBm and  $1.771 \times 10^{-8}$  @ -33 dBm separately.

Then the OAF relaying-assisted OOK system is simulated. The parameter settings and the data rate remain unchanged. The optical power at the relaying node (output of VOA1)  $P_r^{IN}$  is separately fixed at -30 dBm, -31 dBm and -33.4 dBm. The corresponding BERs at the receiver are recorded under different optical power  $P_R^2$  and plotted in Fig. 3(d). The obtained BER curves demonstrate that the higher optical power  $P_r^{IN}$  the relaying node receives, the better BER the receiver performs. Besides, taking the BER level of  $10^{-7}$  as reference, the no-relaying system requires  $P_R^1 = -33.4$  dBm at the receiver (the red w/o relaying line), while the relaying-assisted system requires  $P_R^2 = -32.8$  dBm at the receiver, with the input power of the relaying node  $P_r^{IN}$  maintained at -33.4 dBm.

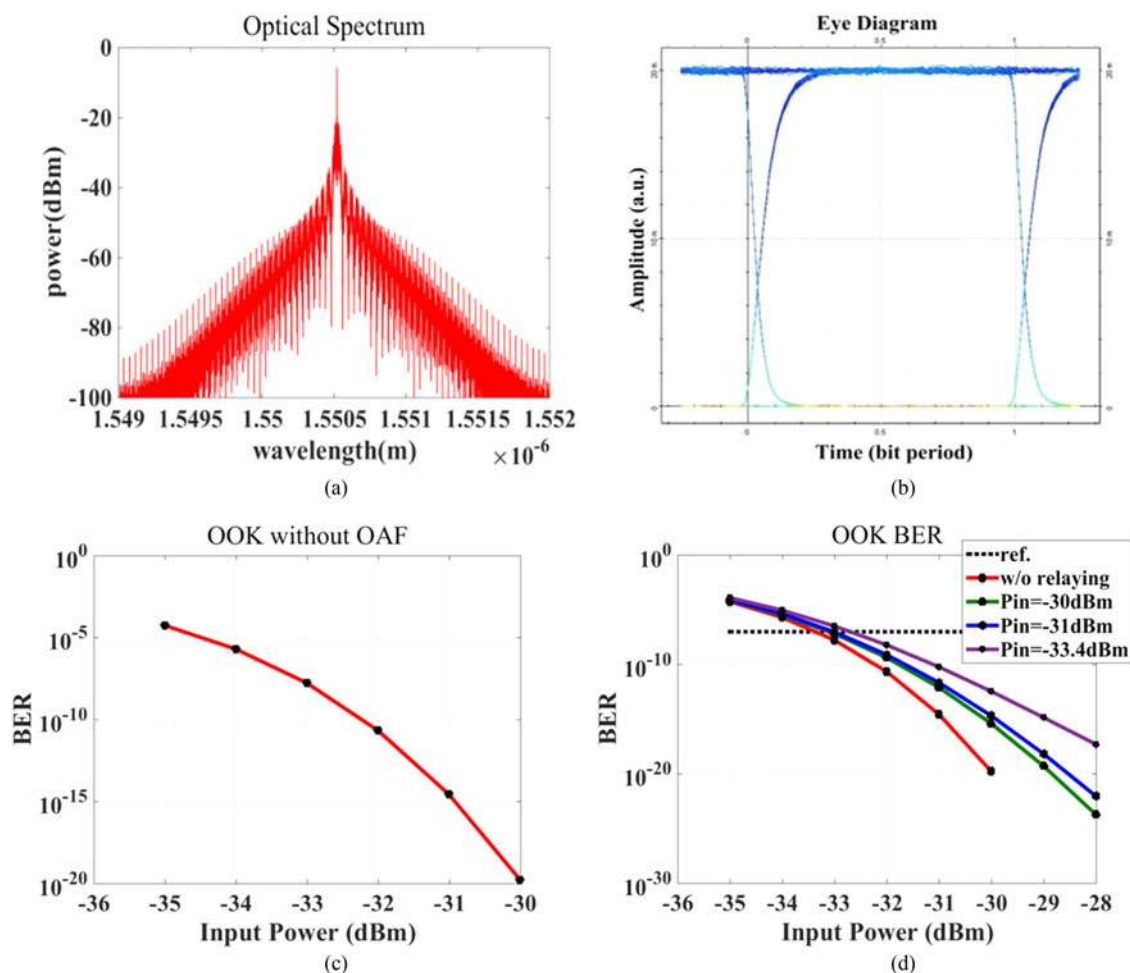


Fig. 3. Simulation results of OOK system. (a) optical spectrum, (b) eye diagram, (c) no-relaying system BER curve and (d) OAF relaying BER curves.

From the above comparison we can conclude that compared to the no-relaying system, the RSL (defined as  $RSL = P_R^2 - P_R^1$  at the same BER reference) for the relaying-assisted system is less than 1 dB at the BER level of  $10^{-7}$ , while the transmission distance is doubled. Furthermore, in the relaying-assisted system, the required input power  $P_R^2$  at the receiver can lower to  $-33$  dBm when the optical power  $P_r^{IN}$  at the relaying node increases to  $-31$  dBm or higher.

**3.1.2 Experimental Results:** Then we perform experiments to verify the simulation results, and the experimental setup is illustrated in Fig. 2. A 5-Gb/s non-return-to-zero (NRZ) OOK optical signal is generated by modulating a  $(2^{15}-1)$ -long PRBS data, originating from a pattern generator (PG, Anritsu, MP1800A), onto the CW laser light (TeraXion, PS-TNL) with a standard MZM (Fujitsu, FTM7938EZ), and a BC is used to guarantee the MZM be properly biased. The OOK signal is then launched into 50-m long atmospheric channel and received by the relaying node. At the relaying node, the optical power is further attenuated by VOA1 (EXFO, FVA-3150) to simulate the longer transmission distance in practical system, and an EDFA (Keopsys, CEFA-C-HG) and a tunable OBPF (Santac, OTF-930) are employed to relay the degraded optical signal. Then the relayed signal travels another 50-m free space channel to arrive at the receiver. At the receiver, VOA2 (EXFO, FVA-3150) is firstly used to simulate the actual longer distance transmission, then the input signal is amplified by an EDFA (Keopsys, CEFA-C-HG) and filtered using an optical filter (Yenista,

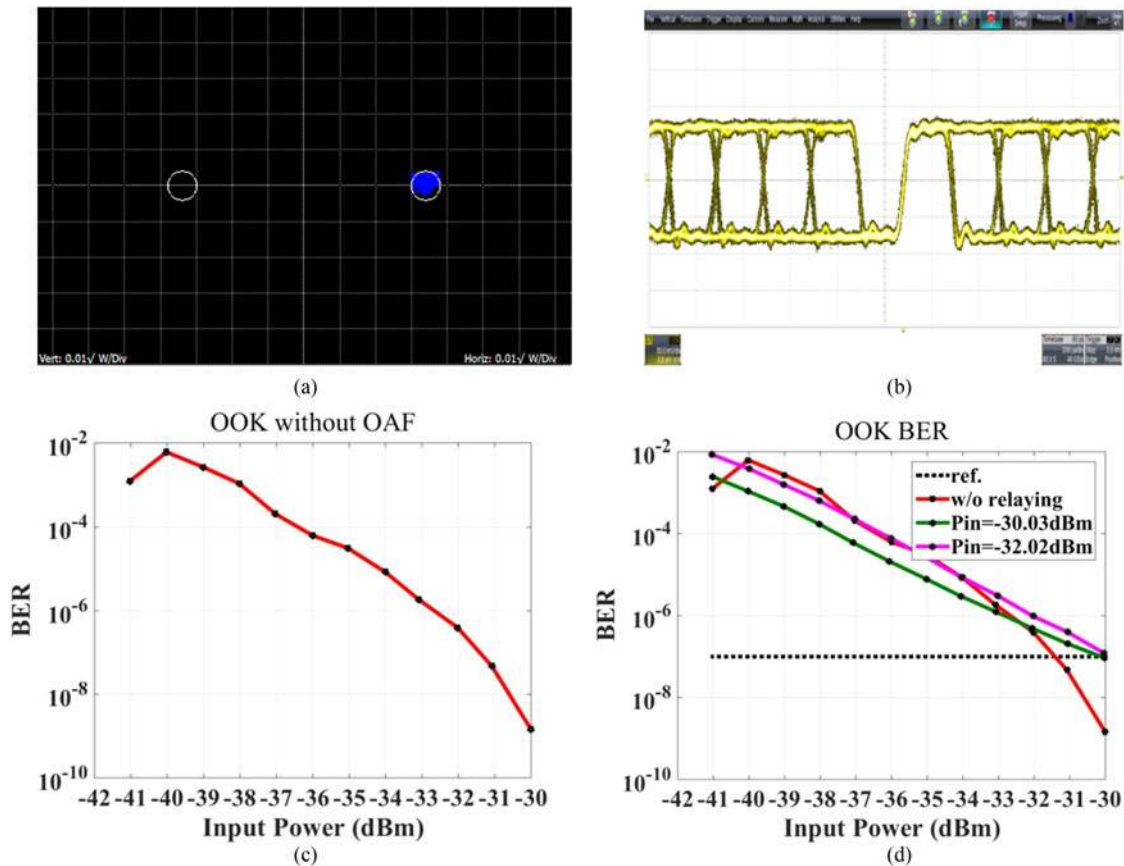


Fig. 4. Experimental results of OOK signal. (a) constellation, (b) eye diagram, (c) no-relaying system BER curve and (d) OAF relaying BER curves.

XTA-50), and finally detected by a PD ( $u^2t$ , XPDV2120R). The vital parameters of the antennas (OZ Optics, HPUCO-23) deployed in the system are listed in Table 1. The received optical power at the relaying node  $P_r^{IN}$  and at the receiver  $P_R^1$ ,  $P_R^2$  are separately monitored by optical power meters (JDSU, OLP-55) through 3 dB beam-splitters.

Similarly to the simulation process, firstly we perform the no-relaying experiment, and the obtained constellation (Tektronix, MSO 73304DX), the eye diagram (Lecroy, SDA8252i) and the receiving BERs (Agilent, N4962BERT) are illustrated in Fig. 4. From Fig. 4(c) we can find that in no-relaying system, the BERs of the OOK signal are  $3.92 \times 10^{-7}$  @  $-32.02$  dBm and  $1.47 \times 10^{-9}$  @  $-30.03$  dBm. Then the experiments with OAF relaying are carried out. The received optical power  $P_r^{IN}$  at the relaying node are separately fixed at  $-32.02$  dBm and  $-30.03$  dBm. The corresponding BERs at different optical power  $P_R^2$  of the receiver are recorded and plotted in Fig. 4(d). It can be seen that taking the BER level of  $10^{-7}$  as the reference, the no-relaying system requires  $P_R^1 = -31.5$  dBm at the receiver (the red w/o relaying line), whereas the relaying-assisted system requires  $P_R^2 = -30.12$  dBm at the receiver, with the optical power at the relaying node  $P_r^{IN} = -30.03$  dBm. However, this requirement will change to  $-30.04$  dBm at the receiver when the optical power at the relaying node lower to  $-32.02$  dBm.

From the above experimental results we can infer that at the BER reference of  $10^{-7}$ , the OAF relaying node can double the transmission range, while the required optical power at the receiver increase from  $P_R^1 = -31.5$  dBm to  $P_R^2 = -30.04$  dBm c to the no-relaying system. Hence the RSL caused by OAF relaying is less than 1.5 dB for OOK system.



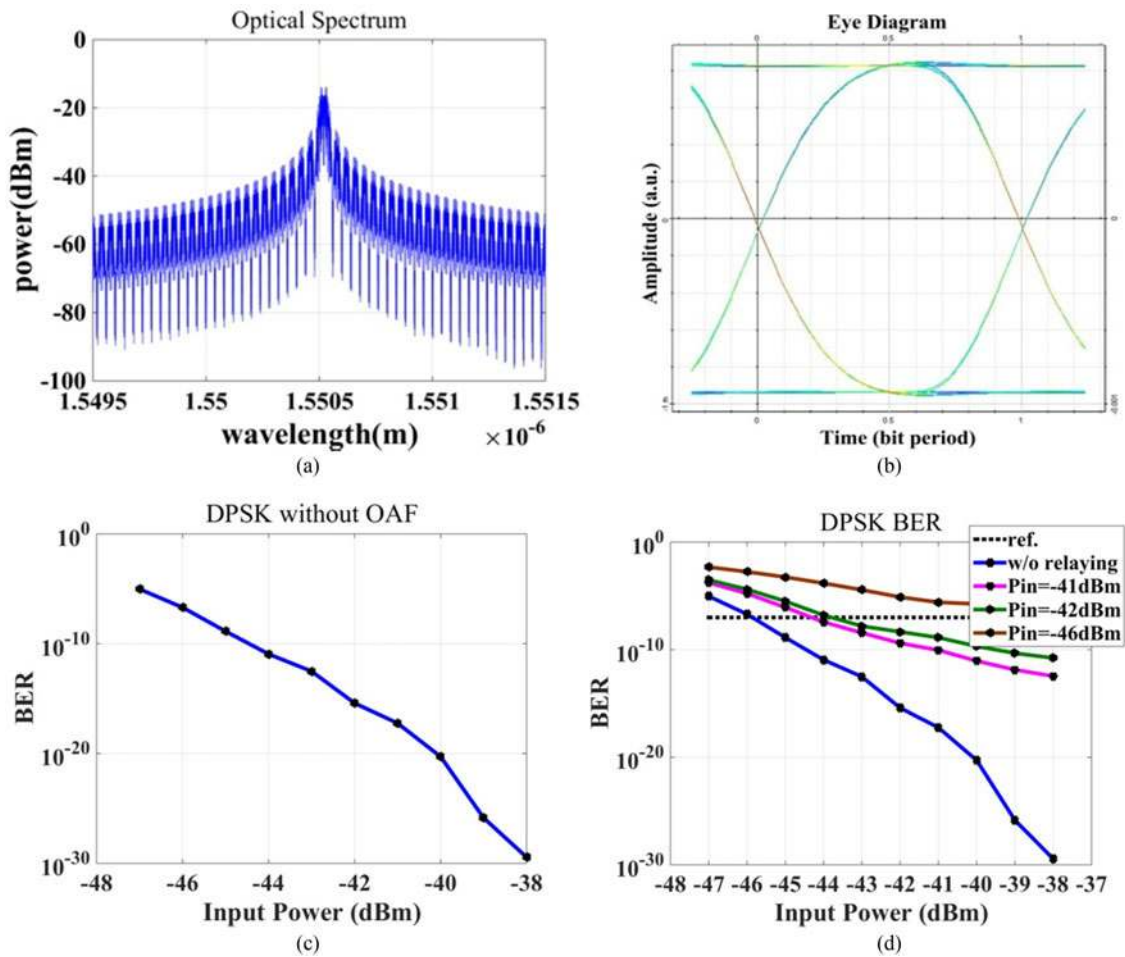


Fig. 5. Simulation results of DPSK signal. (a) optical spectrum, (b) eye diagram, (c) no-relaying system BER curve and (d) OAF relaying BER curves.

### 3.2 DPSK Modulation

We also carry out simulations and experiments on DPSK dual-hop FSO system. In the DPSK system, setup in the simulations and the experiments keeps unchanged compared to OOK system, excepting that the differential encoding part (inset (a) of Fig. 2) is turned on before the data modulation.

**3.2.1 Simulation Results:** Similarly we carry out the no-relaying system simulation for the DPSK system firstly. By changing the optical power through VOA2, we record the receiver's BERs under different optical power  $P_R^1$  and plot the BER curves. The results are demonstrated in Fig. 5. As shown in Fig. 5(c), the receiving BERs in the no-relaying DPSK transmission system are  $5.756 \times 10^{-18}$  @  $-41$  dBm,  $3.868 \times 10^{-16}$  @  $-42$  dBm and  $1.996 \times 10^{-7}$  @  $-46$  dBm, respectively. Then the OAF relaying-assisted system is simulated. With the received optical power at the relaying node  $P_r^{IN}$  separately fixed at  $-41$  dBm,  $-42$  dBm and  $-46$  dBm, the corresponding BERs at the receiver under different optical power  $P_R^2$  are recorded and plotted in Fig. 5(d). In the same way, the BER level of  $10^{-7}$  is chosen as the reference. In the no-relaying system, the required input power  $P_R^1$  at the receiver is  $-46$  dBm (the blue w/o relaying line), meanwhile in the relaying-assisted system, the receiver requires  $P_R^2 = -37.5$  dBm optical power with the relaying node input power  $P_r^{IN}$  kept at  $-46$  dBm. However, the requirement for  $P_R^2$  can lower to  $-44$  dBm when the input power  $P_r^{IN}$  at the relaying node increasing to  $-42$  dBm and  $-41$  dBm.

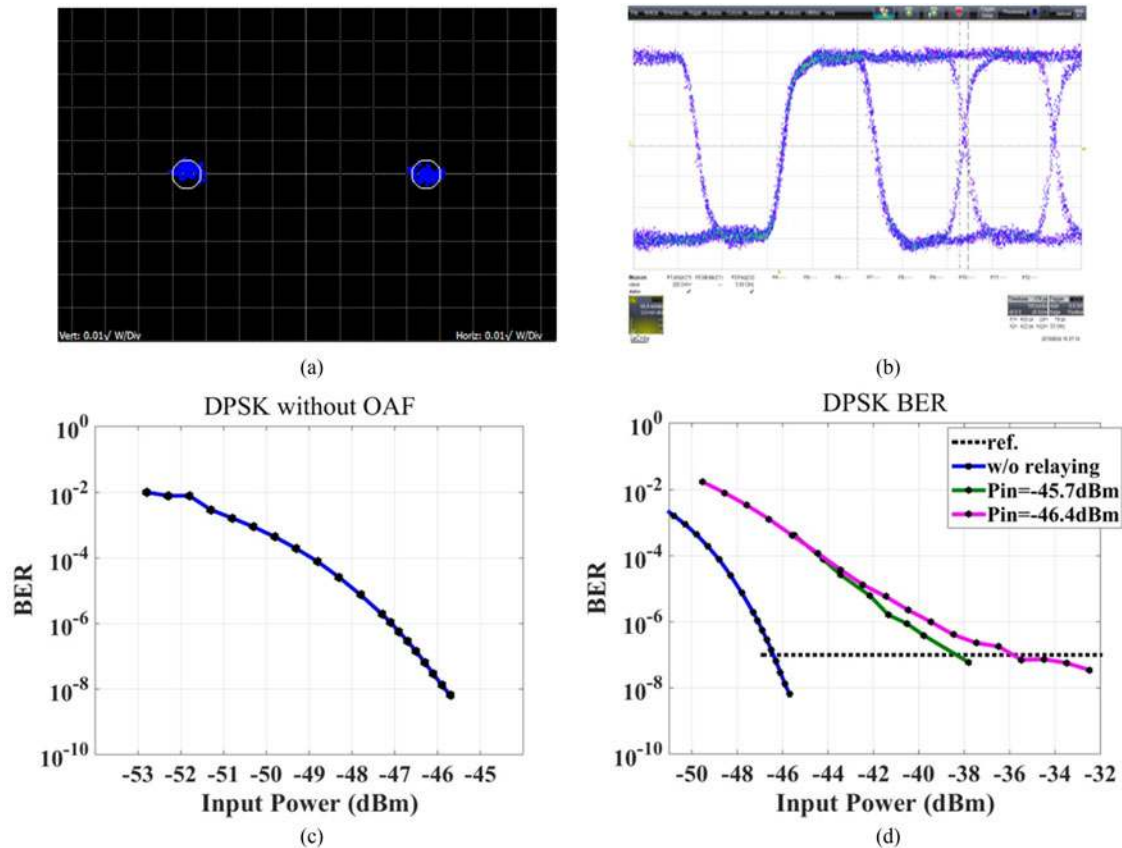


Fig. 6. Experimental results of DPSK signal. (a) constellation, (b) eye diagram, (c) no-relaying system BER curve and (d) OAF relaying BER curves.

The above comparison reaches a conclusion that compared to the no-relaying system, the OAF relaying-assisted system with DPSK modulation gets more than 8 dB RSL to double the transmission distance.

**3.2.2 Experimental Results:** Then we perform experiments to verify the simulation results. As shown in the Fig. 2, a 5-Gb/s NRZ-DPSK signal is generated by applying the differential encoder to the PRBS data before modulation, and adjusting the BC output voltage to keep the modulator biased at the minimum point. At the receiver, after pre-amplifying and filtering, the DPSK signal is demodulated by a 1-bit DI (Kylia, MINT-1550) and balanced detected by a BPD ( $u^2t$ , BPRV2125A). For the no-relaying system, the measured constellation, eye diagram and receiver BERs at different optical power  $P_R^1$  are demonstrated in Fig. 6. From Fig. 6(c) we can see that in no-relaying system, the receiving sensitivities at the receiver are  $1.41 \times 10^{-7}$  @  $-46.4$  dBm and  $6.44 \times 10^{-9}$  @  $-45.7$  dBm.

Subsequently the OAF relaying-assisted experiments are performed, and the optical powers at the relaying node  $P_r^{IN}$  are fixed at  $-45.7$  dBm and  $-46.4$  dBm. At the receiver, the BERs at different optical power  $P_R^2$  are recorded and plotted in Fig. 6(d). With the BER level of  $10^{-7}$  as the comparison reference, we find that for the OAF relaying-assisted system, the required optical power  $P_R^2$  at the receiver is  $-36.5$  dBm while the input power  $P_r^{IN}$  at the relaying node kept at  $-46.4$  dBm. Comparing to the no-relaying system, in which the received power  $P_R^1$  is  $-46.4$  dBm to achieve BER level of  $10^{-7}$ , the OAF relaying-assisted system suffers nearly 10 dBm RSL at the receiver to double the transmission distance. Certainly this requirement can lower to  $P_R^2 = -39.8$  dBm when the received power  $P_r^{IN}$  at the relaying node increases to  $-45.7$  dBm.

### 3.3 Summary

The obtained simulation and experimental results prove that when the OAF relaying is adopted to extend the FSO transmission distance, the DPSK system suffers more RSL than the OOK system. In the simulations, the DPSK system gains more than 8 dB RSL, while the OOK system gets less than 1 dB RSL at the same comparison reference of  $10^{-7}$  BER. Similar results are obtained in the corresponding experiments, the RSL of the OOK dual-hop system is less than 1.5 dB, whereas in DPSK dual-hop system, this value increases nearly to 10 dB, verifying the conclusion we drawn from the simulation results.

## 4. Conclusion

In this paper, we investigate the performance of OAF relaying-assisted dual-hop FSO communication system through simulations and experiments. BERs of OOK and DPSK systems are measured in the no-relaying system and the relaying-assisted system, and corresponding RSLs, to the best of the authors' knowledge, are firstly studied through simulations and experiments separately. A good agreement is demonstrated between the simulations and experiments. Meanwhile, this is the first comparison of RSLs between OOK and PSK in the all-optical OAF-assisted FSO system.

It has been known that DPSK with a balanced receiver has a 3 dB receiving sensitivity advantage over OOK. Nevertheless, when the OAF relaying node are adopted to extend the FSO transmission distance, the DPSK system unexpectedly suffers more RSL than OOK system at the BER level of  $10^{-7}$ . The simulation results show that the RSL of the OOK dual-hop system is less than 1 dB, which in the DPSK system is more than 8 dB. The obtained experimental results, in which the RSL for OOK system is less than 1.5 dB, whereas in DPSK system the RSL increases to nearly 10 dB, verify the simulation conclusion. The results mean that DPSK system, comparing to OOK, is more affected by the ASE noise and background radiation introduced by OAF relaying node. This is particularly instructive when both the receiving sensitivity and the transmission distance matter in FSO system. In the OOK dual-hop system, the OAF relaying node can be simply placed between two identical distance, with the receiving sensitivity nearly unchanged. While in the DPSK dual-hop system, the OAF relaying node should be carefully positioned, and the distance after the relaying node should be much shorter than that before the relaying node to guarantee the receiving sensitivity.

---

## References

- [1] P. Saxena, A. Mathur, and M. R. Bhatnagar, "BER performance of an optically pre-amplified FSO system under turbulence and pointing errors with ASE noise," *J. Opt. Commun. Netw.*, vol. 9, no. 6, pp. 498–510, Jun. 2017, DOI: [10.1364/JOCN.9.000498](https://doi.org/10.1364/JOCN.9.000498).
- [2] Z. N. Chaleshtory, A. Gholami, Z. Ghassemlooy, and M. Sedghi, "Experimental investigation of environment effects on the FSO link with turbulence," *IEEE Photon. Technol. Lett.*, vol. 29, no. 17, pp. 1435–1438, Sep. 1, 2017, DOI: [10.1109/LPT.2017.2723569](https://doi.org/10.1109/LPT.2017.2723569).
- [3] M. A. Khalighi and M. Uysal, "Survey on free space optical communication: A communication theory perspective," *IEEE Commun. Surveys Tuts.*, vol. 16, no. 4, pp. 2231–2258, Fourth Quarter 2014.
- [4] A. Mansour, R. Mesleh, and M. Abaza, "New challenges in wireless and free space optical communications," *Opt. Lasers Eng.*, vol. 89, pp. 95–108, Feb. 2017, DOI: [10.1016/j.optlaseng.2016.03.027](https://doi.org/10.1016/j.optlaseng.2016.03.027).
- [5] R. K. Singh, Karmeshu, and S. Kumar, "A novel approximation for K distribution: Closed-Form BER using DPSK modulation in free-space optical communication," *IEEE Photon. J.*, vol. 9, no. 5, Oct. 2017, Art. no. 7906817, DOI: [10.1109/JPHOT.2017.2746763](https://doi.org/10.1109/JPHOT.2017.2746763).
- [6] NASA, "Hello, World! NASA beams video from space station via laser," 2014. [Online]. Available: <https://www.nasa.gov/press/2014/june/nasa-beams-hello-world-video-from-space-via-laser/>.
- [7] B. V. Oaida *et al.*, "Optical link design and validation testing of the Optical Payload for Lasercomm Science (OPALS) system," in *Proc. SPIE*, vol. 8971, 2014.
- [8] S. Tingting, J. Ma, and L. Tan, "Lunar Laser communication demonstration in USA: Terminal design," *Laser Optoelectron. Prog.*, vol. 51, no. 5, 2014, Art. no. 050003, DOI: [10.3788/LOP51.050003](https://doi.org/10.3788/LOP51.050003).
- [9] T. Song, M-W. Wu, and P-Y. Kam, "Mitigation of the background radiation for free-space optical IM/DD systems," *IEEE Commun. Lett.*, vol. 22, no. 2, pp. 292–295, Feb. 2018.
- [10] S. Arnon and N. S. Kopeika, "Laser satellite communication network-vibration effect and possible solutions," *Proc. IEEE*, vol. 85, no. 10, pp. 1646–1661, Oct. 1997.

- [11] N. A. M. Nor, Z. Ghassemlooy, S. Zvanovec, and M. A. Khalighi, "Performance analysis of all-optical amplify-and-forward FSO relaying over atmospheric turbulence," in *Proc. IEEE Student Conf. Res. Develop.*, 2015, pp. 289–293.
- [12] M. Safari and M. Uysal, "Relay-assisted free-space optical communication," *IEEE Trans. Wireless Commun.*, vol. 7, no. 12, pp. 5441–5449, Dec. 2008, DOI: [10.1109/T-WC.2008.071352](https://doi.org/10.1109/T-WC.2008.071352).
- [13] T. Tsiftsis, H. Sandalidis, G. Karagiannidis, and N. Sagias, "Multihop free-space optical communications over strong turbulence channels," in *Proc. IEEE Int. Conf. Commun.*, 2006, vol. 6, pp. 2755–2759.
- [14] M. Karimi and M. Nasiri-Kenari, "Free space optical communications via optical amplify-and-forward relaying," *J. Lightw. Technol.*, vol. 29, no. 2, pp. 242–248, Jan. 2011, DOI: [10.1109/JLT.2010.2102003](https://doi.org/10.1109/JLT.2010.2102003).
- [15] M. T. Dabiri and S. M. S. Sadough, "Performance analysis of all-optical amplify and forward relaying over log-normal FSO channels," *J. Opt. Commun. Netw.*, vol. 10, no. 2, pp. 79–89, Feb. 2018, DOI: [10.1364/JOCN.10.000079](https://doi.org/10.1364/JOCN.10.000079).
- [16] M. A. Kashani, M. M. Rad, M. Safari, and M. Uysal, "All-Optical amplify-and-forward relaying system for atmospheric channels," *IEEE Commun. Lett.*, vol. 16, no. 10, pp. 1684–1687, Oct. 2012, DOI: [10.1109/LCOMM.2012.082012.121066](https://doi.org/10.1109/LCOMM.2012.082012.121066).
- [17] S. Kazemlou, S. Hranilovic, and S. Kumar, "All-optical multihop free-space optical communication systems," *J. Lightw. Technol.*, vol. 29, no. 18, pp. 2663–2669, Sep. 15, 2011, DOI: [10.1109/JLT.2011.2160615](https://doi.org/10.1109/JLT.2011.2160615).
- [18] E. Bayaki, D. S. Michalopoulos, and R. Schober, "EDFA-based all-optical relaying in free-space optical systems," *IEEE Trans. Commun.*, vol. 60, no. 12, pp. 3797–3809, Dec. 2012, DOI: [10.1109/TCOMM.2012.090512.110198](https://doi.org/10.1109/TCOMM.2012.090512.110198).
- [19] N. A. M. Nor *et al.*, "Experimental investigation of all-optical relay-assisted 10Gb/s FSO link over the atmospheric turbulence channel," *J. Lightw. Technol.*, vol. 35, no. 1, pp. 45–53, Jan. 1, 2017, DOI: [10.1109/JLT.2017.2654878](https://doi.org/10.1109/JLT.2017.2654878).
- [20] L. Li *et al.*, "All-optical regenerator of multi-channel signals," *Nature Commun.*, vol. 8, 2017, Art. no. 884, DOI: [10.1038/s41467-017-00874-0](https://doi.org/10.1038/s41467-017-00874-0).
- [21] P. Guan *et al.*, "Scalable WDM phase regeneration in a single phase-sensitive amplifier through optical time lenses," *Nature Commun.*, vol. 9, 2018, Art. no. 1049, DOI: [10.1038/s41467-018-03458-8](https://doi.org/10.1038/s41467-018-03458-8).
- [22] J. Tan *et al.*, "All-Optical transparent forwarding relay system for interstellar optical communication networks," *IEEE J. Quantum Electron.*, vol. 54, no. 2, Apr. 2018, Art. no. 8000207.
- [23] N. A. M. Nor *et al.*, "Experimental investigation of all-optical relay-assisted 10 Gb/s FSO link over the atmospheric turbulence channel," *J. Lightw. Technol.*, vol. 35, no. 1, pp. 45–53, Jan. 2017.
- [24] J. Horwath *et al.*, "Test results of error-free bidirectional 10 Gbps link for air-to-ground optical communications," in *Proc. SPIE*, 2018, vol. 10524, DOI: [10.1117/12.2306191](https://doi.org/10.1117/12.2306191).
- [25] H. Ivanov, E. Leitgeb, T. Plank, P. Bekhrad, and T. Mitsev, "Link budget optimization of free space optical systems in relation to the beam diverging angle," in *Proc. 13th Int. Conf. Telecommun.*, 2018, pp. 1–5.